

UNCLASSIFIED

Defense Technical Information Center
Compilation Part Notice

ADP010913

TITLE: New Statistical Textural Transforms for
Non-Stationary Signals; Application to
Generalized Multifractal Analysis

DISTRIBUTION: Approved for public release, distribution unlimited

This paper is part of the following report:

TITLE: Paradigms of Complexity. Fractals and
Structures in the Sciences

To order the complete compilation report, use: ADA392358

The component part is provided here to allow users access to individually authored sections of proceedings, annals, symposia, ect. However, the component should be considered within the context of the overall compilation report and not as a stand-alone technical report.

The following component part numbers comprise the compilation report:

ADP010895 thru ADP010929

UNCLASSIFIED

NEW STATISTICAL TEXTURAL TRANSFORMS FOR NON-STATIONARY SIGNALS; APPLICATION TO GENERALIZED MULTIFRACTAL ANALYSIS

ANTOINE SAUCIER

CERCA, 5160 boul. Décarie, bureau 400, Montréal (Québec), Canada H3X 2H9,
e-mail: antoine@cerca.umontreal.ca

JIRI MULLER

Institutt for Energiteknikk, P.O. Box 40, N-2007 Kjeller, Norway, e-mail: jiri@ife.no

We introduce a method to generate statistical textural transforms that improves the treatment of non-stationarity and leads to a sharper detection of the boundaries between distinct textures (texture segmentation). This method is based on a sliding window processing with fixed size. The basic idea proposed by the authors is to readjust the measuring window around each pixel so as to maximize homogeneity. We use this method with the dimensions $D_n(q)$ that are derived from the Generalized Multifractal Analysis formalism, to show that the $D_n(q)$ s can detect and quantify departures from multifractality, while providing the analogue of the classical generalized dimension if the measure is multifractal.

1 Introduction

We propose a method to generate statistical textural transforms that improves the treatment of non-stationarity. Our goal is to improve the quality of the texture segmentations¹ that can be obtained from textural transforms based on a simple sliding window processing². In this context, one usually assumes implicitly that the signal is locally stationary and then proceeds directly with parameter estimation. This assumption is usually not legitimate for every part of the signal. Indeed, there are usually some windows that are not homogeneously textured, which can result in unreliable texture parameters. We propose a more careful treatment of the local homogeneity that leads to significant segmentation improvements. We also apply our method to the generalized multifractal analysis (GMA) representation³ to show that the generalized dimensions $D_n(q)$ can detect and quantify departures from multifractality, while providing the analogue of the classical generalized dimension $D(q)$ if the measure is multifractal.

2 Non-Stationarity and the legitimacy of statistical texture parameters

For a 1D signal $S(x)$, a resolution preserving⁴ *textural transform* associates to each point of the x -axis a number that quantifies an aspect of the local variations of $S(x)$ in the neighborhood of x . The texture parameter associated to a point x_0 is often computed from an interval *centered* on x_0 such as $[x_0 - L_w / 2, x_0 + L_w / 2]$, where L_w is the *window size*. In this case, we talk about a *sliding window processing* of the signal. In the following, the function giving a texture parameter as a function of x will be called a *texture log*. For *statistical* textural transforms, the parameter computed from the signal is statistical in nature.

Texture logs can be used to detect variations in the local statistics of a signal. The signals of interest are therefore typically *non-stationary*. In this paper, we focus on signals for which the textural variations are either slow or abrupt. In other words, we consider signals that are almost *piecewise stationary*, i.e. nearly stationary on consecutive disjoint

intervals. In this context, the presence of discontinuities at the boundaries of adjacent stationary zones raises questions with respect to the sliding window processing. Consider for instance the simple signal shown in Fig. 1. This signal is composed of four segments of equal size (500 points). For each segment, the signal was constructed by adding uniform random deviates (uncorrelated and uniform on $[0, 1]$) to either a constant or to a slow linear trend. This signal will be regarded as approximately piecewise stationary.

To start with a very simple example of statistical texture parameter, let us suppose that we want to obtain the *mean* texture log of this signal with a sliding window processing, i.e. we compute for each point the arithmetic average of the window centered on this point (Fig. 2). As long as the window lies entirely within one of the four segments, then the data contained in this window is approximately stationary (i.e. statistical *homogeneity* within the window) and it makes sense to compute the mean from the window. However, for windows that *overlap* between two segments, the situation is different. Indeed, such windows then contain two subsets of data that have different and *inconsistent* probability distributions. From a statistical standpoint, it is not legitimate or meaningful to blend two statistically inconsistent samples and then compute a mean. Indeed, the mean obtained is *not representative* of any of the two statistical ensembles. This simple example suggests that *a statistical texture parameter should be computed only for windows that are sufficiently homogeneous statistically*^a, otherwise the resulting parameter is neither representative nor statistically meaningful.

This leads to the problem of measuring the statistical homogeneity of a window. We will use the simple approach that consists in splitting the window in two disjoint subsamples of equal size, and then to apply a statistical test to compare the distributions obtained from each half. For this comparison, we will use the *Kolmogorov-Smirnov* statistical test that gives the probability *prob1* that the two samples were drawn from the same distribution. To include a sensitivity to 2-point statistics, we will also compare the distributions of the 2-point products $s(i)s(i+n)$ ($n = 0, 1, 2, \dots$) obtained from each half window (here $s(i)$ denotes the value of the signal at point i). For each n , the Kolmogorov-Smirnov test gives a probability *prob2(n)* that the two samples were drawn from the same distribution. We then define a *homogeneity index* by

$$\text{Homogeneity Index} = \text{Min} \{ \text{prob1}, \text{prob2}(1), \text{prob2}(2), \dots \}$$

i.e. our homogeneity index is the most pessimistic probability obtained from the statistical comparisons involving one and two point statistics.

In Fig. 2 we plotted the mean texture log together with the homogeneity index for the sample of Fig. 1 (window size = 50 points). The homogeneity index drops to extremely small values at the discontinuities occurring at $i = 500$ and 1000 . Around these locations, the texture log takes the form of a linear transition between two plateaus. Elsewhere, the homogeneity index is large enough to confirm the approximate stationarity of the signal. In our opinion, the windows for which the homogeneity index is very low should not be used to estimate a statistical parameter. For this reason, we propose to revise the idea of a textural transform strictly based on a sliding window processing

^a In this paper, we will use the expressions *statistical homogeneity* and *stationarity* as synonymous.

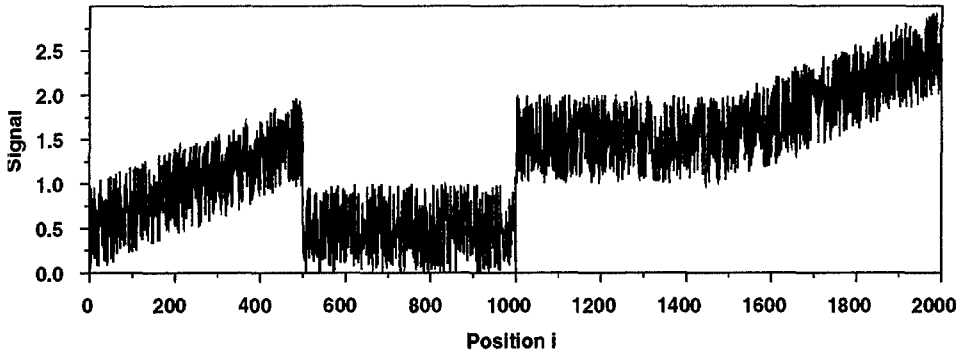


Figure 1: An example of a signal that is approximately piecewise stationary.

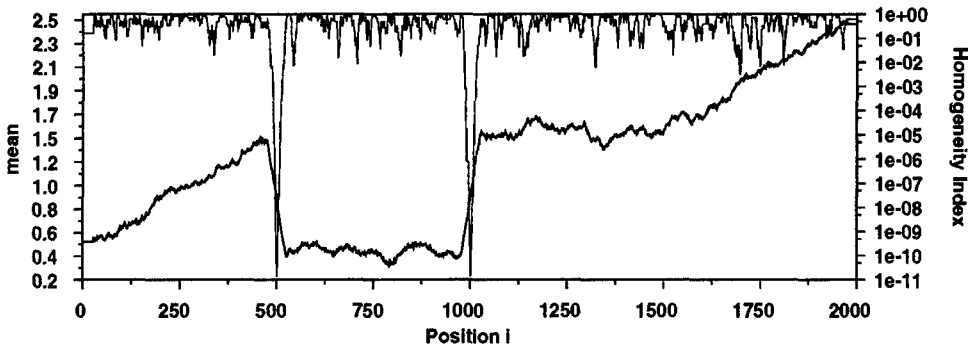


Figure 2: Mean texture log and homogeneity index (the stalactite looking signal on top).

3 A segmentation-oriented strategy for textural transforms

On one hand, the idea of associating a texture parameter computed from a window to the center of this window is not as natural as it might seem *a priori*. Indeed, a texture parameter is associated with a window, not with a point. In reality, any point belonging to this window is equally entitled to receive this texture parameter, especially if every point has contributed equally to its computation. On the other hand, the whole purpose of a texture log is to detect spatial variations of the local texture. From this standpoint, it is desirable that the spatial variations of the texture log reflect the spatial variations of the statistics of the underlying signal. Attributing the texture parameter to the window center is a simple way to obtain this dependence.

In this paper, we adopt the standpoint according to which the textural transform is to be used primarily for segmentation purposes, i.e. to divide the signal into zones having similar statistics. In other words, the textural transform is regarded as a first step toward segmentation. It follows from this standpoint, for instance, that if there is an abrupt transition between two zones, then the texture log should also exhibit an abrupt transition. It also follows that it is necessary to associate a texture parameter with each point of the signal, i.e. the textural transform should be resolution preserving, which is not possible if only the window centers are considered (i.e. sliding window processing). Finally, a statistical textural transform should be based only on windows that are reasonably homogeneous statistically, as far as possible.

To satisfy these guidelines, let us examine again the abrupt transition between two zones, (Figs. 1-2). If the window considered is homogeneous enough, then there is no statistical inconsistency and we choose to adopt the usual sliding window method, i.e. we

attribute to a point x the texture parameter of the window that is centered on x . However, if the window *overlaps* between two different zones A and B , then the window is statistically inconsistent and we want to modify the usual sliding window strategy. If the point x considered belongs to zone A , then it seems natural to attribute to x the texture parameter of a window that both contains x and that lies entirely within the zone A (see point x_3 in Fig. 3). Indeed, x belongs to zone A and should therefore be attributed a texture parameter that is representative of this zone. *From this standpoint, the problem is to select for each point x the most appropriate window among all the windows that contain x .*

We propose the following window selection rule for a given point x . Among all the windows that contain x and that have a satisfactory homogeneity (if they exist) we select the window that is most centered on x , i.e. the window for which the distance between its center y and x is minimum. If none of the windows containing x is homogeneous enough, then we simply select the most homogeneous window containing x . Notice that in general there will be two windows at an equal distance $|y - x|$ of x , the left and the right window. To make the choice unambiguous, we select the most homogeneous of these two windows. It is emphasized that if the signal is homogeneous enough, then our definition reduces to the usual sliding window approach. However, if the homogeneity is not acceptable, then our definition forces the windows to "stay away" from discontinuities. We will refer to this approach as the sliding window method with homogeneity correction, or *SWMHC*.

Let us examine a few consequences of our homogeneity correction. If x is close^b to the beginning of the signal, then the windows containing x cannot be centered on x (see point x_1 in Fig. 3). If x is away from the boundaries and in a homogeneous zone, then the window selected will be centered on x (point x_2 in Fig. 3). If x is close^c to a boundary between two zones, then the window selected will tend to be entirely within its own zone (point x_3 in Fig. 3).

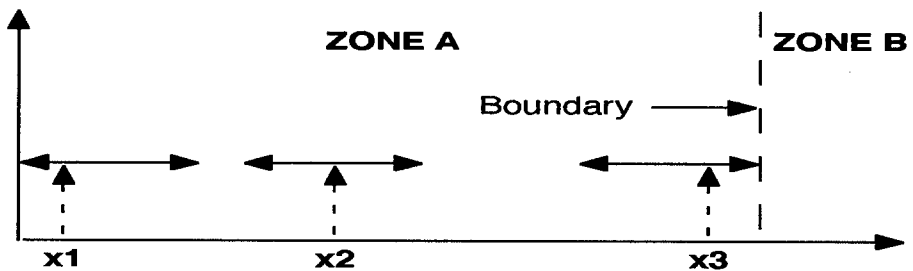


Figure 3: Attribution of windows to each point at the boundary of two zones.

We applied this homogeneity correction algorithm to the signal of Fig. 1, setting the acceptable degree of homogeneity to 0.05 (in statistics, it is usual to reject a hypothesis if the probability associated with a test is smaller than 0.05). It is seen in Fig. 4 that the discontinuities are detected with perfect accuracy, even with a 50-point window size, whereas the rest of the log remains unchanged with respect to Fig. 2. A minimum homogeneity index of 0.05 could be obtained everywhere. Our *SWMHC* has the merit of

^b If the distance between x and the beginning of the signal is smaller than $L_w / 2$, where L_w is the window size.

^c If the distance between x and the boundary of the signal is smaller than $L_w / 2$, where L_w is the window size.

detecting boundaries sharply even for large windows, which is not possible with the usual sliding window method. Our algorithm reduces uncertainties on texture logs because the most inhomogeneous windows are rejected. In the following, the *SWMHC* will be applied to the generalized dimensions $D_n(q)$.

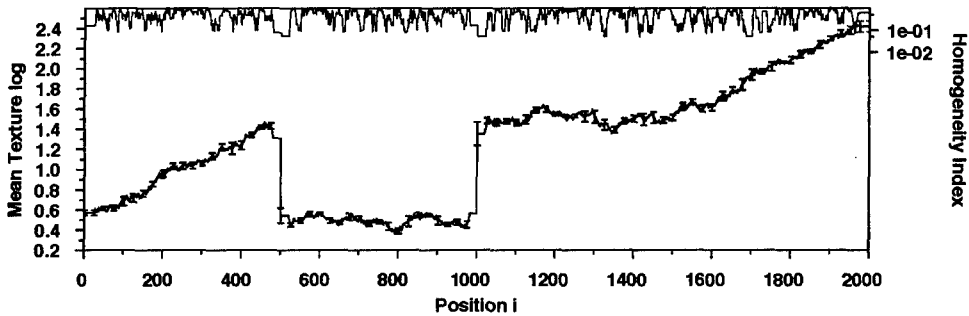


Figure 4: Mean texture log with homogeneity correction. The boundaries at positions 500 and 1000 are detected with perfect accuracy, in spite of the fact that a 50-point window size was used.

It is beyond the scope of this paper to give a comprehensive comparison of our method with the numerous other approaches to texture segmentation, ranging from statistical methods, wavelet based methods and neural networks. In the context of wavelet based methods, for instance, clustering procedures^{6, 7, 8} or detection of sharp transitions over wavelet energy measurements have been used to produce a final segmentation. These algorithms have good experimental performances but rely on ad hoc parameter settings⁹. The same thing can be said of the segmentation methods that combine statistical parameters and neural networks¹⁰ because the network parameters are adjusted on training sets.

One of the first methods used in texture segmentation, and still a major one, is the spatial gray level co-occurrence matrix¹¹. Many authors have approached the problem of texture segmentation with split-and-merge methods combined with co-occurrence matrices^{1, 5}. In this context, one creates homogeneous regions by splitting inhomogeneous regions into smaller regions until a given homogeneity criterion is satisfied in each region (the regions can be rectangular if a regular grid is used, or else they can have other shapes depending on the space partitioning method selected). In comparison, our approach consists in constructing a textural transform based on a fixed window size (and shape), but the window containing a given point can be moved *continuously* to satisfy a homogeneity criterion. In addition, our choice of a statistical test to assess homogeneity gives a certain objectivity to the homogeneity criterion.

For a fixed window size, our method cannot always reach an acceptable degree of homogeneity everywhere. However, reducing sufficiently the window size allows reaching an acceptable homogeneity at all points (as in the split-and-merge algorithm). An appropriate combination of texture logs obtained for different window sizes can be used to produce a multi-resolution texture log with satisfactory homogeneity everywhere.

4 Brief review of the generalized multifractal analysis representation

4.1 Generalized dimensions defined as projections of the generating function on orthogonal polynomials

We summarize here the generalized multifractal analysis (GMA) representation³. The generating function $\chi_q(\delta)$ used in multifractal analysis is a function of two variables q and δ . The parameter q is real and $\delta \geq 0$ is a scale ratio $\delta = \ell / L \leq 1$, where ℓ is a length scale and L is an upper bound on ℓ . Multifractal analysis can be done on the condition that $\chi_q(\delta)$ satisfies the power law property⁷ $\chi_q(\delta) \sim \delta^{\tau(q)}$ in an interval $\delta \in [\delta_{\min}, \delta_{\max}]$ called *scaling range*. With the change of variable $x = -\ln(\delta) \geq 0 \Rightarrow \delta = \exp(-x)$ and the definition $\phi_q(x) \equiv -\ln(\chi_q(\exp(-x)))$, this property can be rewritten in the linear form $\phi_q(x) = \tau_0(q) + \tau_1(q) x$. Many signals cannot be described satisfactorily with this linear model. The GMA representation of $\phi_q(x)$ solves this problem by expanding $\phi_q(x)$ in terms of *orthogonal polynomials* $P_n(x)$ of increasing order n

$$\phi_q(x) = \sum_{n=0}^N \tau_n(q) P_n(x) \tag{1}$$

The model (1) is a generalization of the multifractal model. The coefficients $\tau_n(q)$ are generalizations of $\tau(q)$ ⁷, and $\tau_1(q)$ corresponds to the usual $\tau(q)$ for multifractals. In this paper, we compute $\chi_q(\delta)$ for all the length scales available, i.e. $\ell_n = n, n = 1, 2, \dots, N_x$. The coordinates x take discrete values $x_i, i = 1, 2, \dots, N_x$ and $\phi_q(x)$ is computed for these x_i 's. The $P_n(x)$ s are orthogonal with respect to a scalar product that we define for any two functions f and g by

$$\langle f, g \rangle \equiv \sum_{i=1}^{N_x} w(x_i) f(x_i) g(x_i) \tag{2}$$

where the $w(x_i) > 0$ are weights. A first possibility is to use *unit weights*, i.e. $w(x_i) = 1$ for each i , which gives a larger weight to large scales. Indeed, the density $\rho(x)$ of the x_i 's along the x -axis varies approximately according to $\rho(x_n) = 1/(x_n - x_{n+1}) = 1/\ln(\ell_{n+1}/\ell_n) \approx \ell_n$ and therefore it increases as ℓ_n increases. Another possibility is to use *variable weights* that compensate for the non-uniform density of the x_i 's by choosing $w(x_n) = k / \rho(x_n)$ where the constant k is chosen so that $\sum_i w(x_i) = 1$. This choice results in approximately uniform weighting along the x -axis in the summation (2). It is this second choice that we make in this paper, mostly because it was found to lead to exponents $\tau_n(q)$ that are more sensitive to textural variations.

The $P_n(x)$ s are obtained with a Gram-Schmidt orthogonalization starting with $P_0(x) \equiv 1$ and using iteratively the formula $P_n(x) = x^n - \{\beta_n(0) + \beta_n(1) P_1(x) + \dots + \beta_n(n-1) P_{n-1}(x)\}$. Hence they satisfy $\langle P_n, P_m \rangle = \delta_{n,m} \langle P_n, P_n \rangle$ and the $\tau_n(q)$ s in (1) are defined by

$$\tau_n(q) = \langle P_n, \phi_q \rangle / \langle P_n, P_n \rangle \tag{3}$$

The $\tau_n(q)$'s can be always written in the form $\tau_n(q) = (q-1) D_n(q)$, where the $D_n(q)$'s are formal extensions of the generalized dimensions $D(q)$ ³. The linear component $D_1(q)$ reduces to the generalized dimension $D(q)$ if the measure is multifractal, i.e. if $N = 1$ in eq. (1).

4.2 Definition of the generating function

We define the *measure* of an interval $B_r(\delta)$ of size δ centered on a point r by $p_r(\delta) = \sum_{r_i \in B_r(\delta)} S(r_i)$. To estimate uncertainties on the generating function, we always consider a collection of M equal size samples ($M \geq 2$) drawn from the same statistical ensemble. For a single window in a signal, we split the window into *four disjoint intervals* of the same size that are regarded as four independent samples. Firstly, we define for each of these samples an "individual" generating function by (this form holds only if $p_r(\delta) > 0$, see³)

$$\chi_q(\delta) = \delta^{(q-1)D} \langle [p_r(\delta)]^q \rangle_s / \langle p_r(\delta) \rangle_s^q \quad (4)$$

where D is the dimension of the embedding space, and angle brackets $\langle \dots \rangle_s$ denote a *spatial* average. The denominator of (4) guarantees that $\chi_q(\delta)$ is normalized exactly, i.e. that $\chi_1(\delta) = 1$ for all δ . Secondly, we define the "global" generating function $\hat{\chi}_q(\delta)$ obtained from the M samples by

$$\hat{\chi}_q(\delta) = \frac{1}{M} \sum_{i=1}^M \chi_q^{(i)}(\delta) \quad (5)$$

where $\chi_q^{(i)}(\delta)$ denotes the individual generating function of sample i . The uncertainty on $\hat{\chi}_q(\delta)$ is estimated by taking into account the variations of $\chi_q^{(i)}(\delta)$ from sample to sample, and the corresponding uncertainties on $D_n(q)$ can be derived³ (we assume that the $\chi_q^{(i)}(\delta)$ s are uncorrelated). The error formulas used in this paper are ($\sigma(X)$ denotes the standard deviation of a random variable X)

$$\sigma^2(\phi_q(x)) = \frac{1}{M} \left(\frac{\sigma(\chi_q)}{\langle \chi_q \rangle} \right)^2, \quad \sigma^2(\tau_n(q)) = \langle P_n^2, \sigma^2(\phi_q) \rangle / \langle (P_n, P_n) \rangle^2,$$

$$\sigma(D_n(q)) = \sigma(\tau_n(q)) / |q-1|$$

5 Behavior of the $D_n(q)$ s for a transition between two distinct random binomial measures

Our goal here is to show that the generalized dimension $D_1(1)$ reduces to the classical information dimension $D(1)$ for such archetypal multifractals. The homogeneity index is computed as previously except for one difference: The two samples obtained from each half of the window are normalized by their mean before the statistical tests are done. This choice is partly justified by the fact that the two halves of a binomial measure are statistically identical only if each half of the measure is individually normalized.

We construct the random binomial measures as usual. Initially, a unit mass is assigned to the interval $[0, 1]$. In the first step, the unit interval is split in two halves

$[0, 1/2]$ and $[1/2, 1]$. The first interval receives a random fraction $W_{1,1}$ of the mass, where $0 \leq W_{1,1} \leq 1$, while the second interval receives a mass $1 - W_{1,1}$. In the next steps this splitting procedure is repeated in a self-similar manner: In the step $n+1$, interval i , $[(i-1)(1/2)^n, i(1/2)^n]$ of size $\delta_n = (1/2)^n$ and mass $p_i(n)$, is split in two halves receiving the masses $p_{i,1}(n+1) = W_{n,i} p_i(n)$ and $p_{i,2}(n+1) = (1 - W_{n,i}) p_i(n)$, where $W_{n,i}$ is a random variable ($1 \leq i \leq 2^n$). The multipliers $W_{n,i}$ satisfy $0 \leq W_{n,i} \leq 1$ and are identically distributed and mutually independent random variables. We choose here multipliers that take two values w_1 and $w_2 = 1 - w_1$ with equal probability. The signal examined (Fig. 5) is composed of two adjacent binomial measures with parameters $w_1 = 0.25$ and $w_1 = 0.35$, 1024 points each ($n = 10$, i.e. 10 iterations). Each measure was normalized to get a unit root mean square.

We first consider in Fig. 6 the $D_I(I)$ texture log obtained with a window size of 128 points, a maximum box size of 32 points and no homogeneity correction. The dashed lines represent the theoretical values of $D(I)$ for the two binomial measures (we get $D(I) = 0.811$ and 0.934 with $D(I) = -w_1 \log_2(w_1) - w_2 \log_2(w_2)$). $D_I(I)$ fluctuates around the theoretical value of $D(I)$ on both sides, which shows that the GMA representation is consistent with the usual description of multifractals. It can be noticed that $D_I(I)$ oscillates a little below $D(I)$, though the difference is small, which can be explained by the fact that our generating function $\Phi_q(x)$ is not perfectly linear for the binomial measure. The homogeneity index drops to very small values at the boundary between the two measures, located at position 1024. Within each zone, the homogeneity index is relatively large but sometimes drops to small values. This occasional lack of homogeneity results from the fact that the statistical self-similarity of the binomial measure holds exactly only if the two intervals compared with the statistical test match exactly the construction grid of the measure, which is usually not the case.

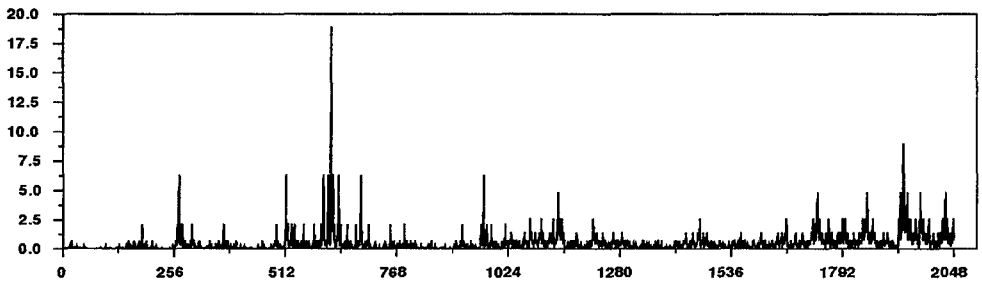


Figure 5: Two adjacent binomial measures.

We recomputed the $D_I(I)$ texture log of Fig. 6 with the homogeneity correction at level 0.05 (Fig. 7). This level was achieved at about 75% of locations, but the level 0.04 is reached almost everywhere. The transition between the two measures is sharp and its location exact, in spite of a window size of 128 points. The amplitude of the fluctuations is reduced by the homogeneity correction. Plateaus are formed, which is a characteristic property of the homogeneity correction. Higher order dimensions, starting with $D_2(I)$, were found to be too small to be distinguished unambiguously (taking into account error bars). This is expected because the function $\Phi_q(x)$ is almost perfectly linear for such binomial measures.

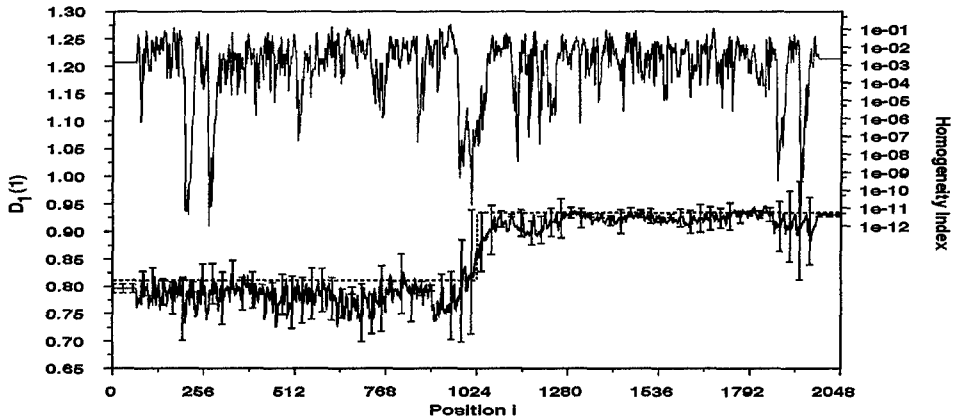


Figure 6: $D_1(I)$ texture log. The stalactite looking curve on top is the homogeneity index.

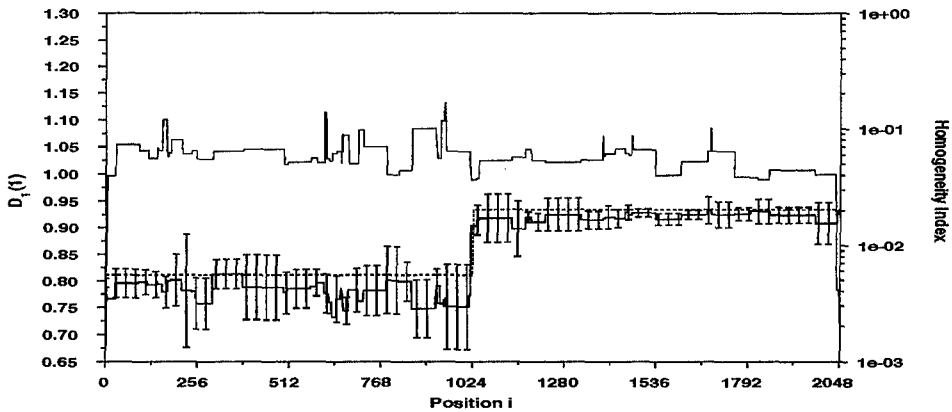


Figure 7: $D_1(I)$ texture log of Fig. 5 with homogeneity correction at level 0.05.

6 Behavior of the $D_n(q)$ s for a transition between a binomial measures and a non self-similar measure

In this section, we show that the GMA representation can be used to detect and quantify *departures from self-similarity*, while providing an analogue of the generalized dimension even if the measure is not self-similar. We examine the GMA texture logs for a transition between a random binomial measure with $w_1 = 0.3$ to a *non self-similar* measure. The latter is constructed by making the factor w_1 vary with the step index n (with the multiplicative process described in section 5.1). Our non self-similar measure was obtained with the following values of $w_1(n)$ ($n=1,2,\dots,10$): $\{0.32, 0.27, 0.28, 0.38, 0.25, 0.25, 0.42, 0.40, 0.11, 0.11\}$. The total measure is obtained by sticking together this measure with the binomial measure (Fig. 8).

The two measures are distinguished clearly by $D_1(I)$ (Fig. 9) and the homogeneity correction again results in a sharp detection of the boundary (Fig. 10). The $D_2(I)$ texture log (Fig. 11) shows a marked transition between the two measures. Indeed, $|D_2(I)|$ is small on the side of the binomial measure (left), and then becomes larger on the side of the non self-similar measure (right). A larger $|D_2(I)|$ indicates a larger deviation of $\Phi_q(x)$ from a straight line, to be expected for a non multifractal.

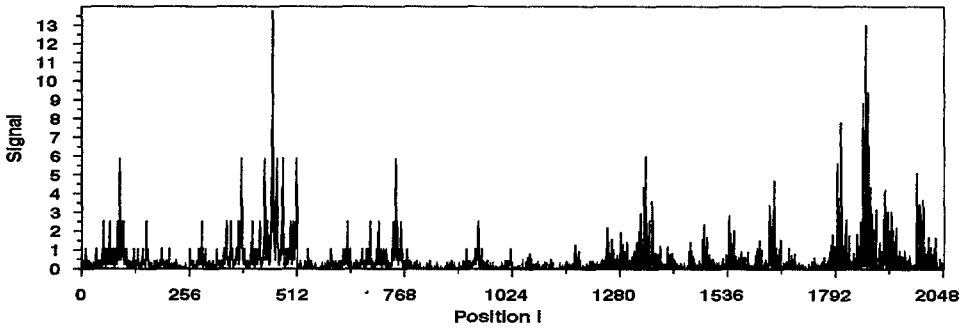


Figure 8: The first half sample is a random binomial measure with $w_1 = 0.3$. The second half of the sample has been built with a multiplicative process where w_1 varies with the step index.

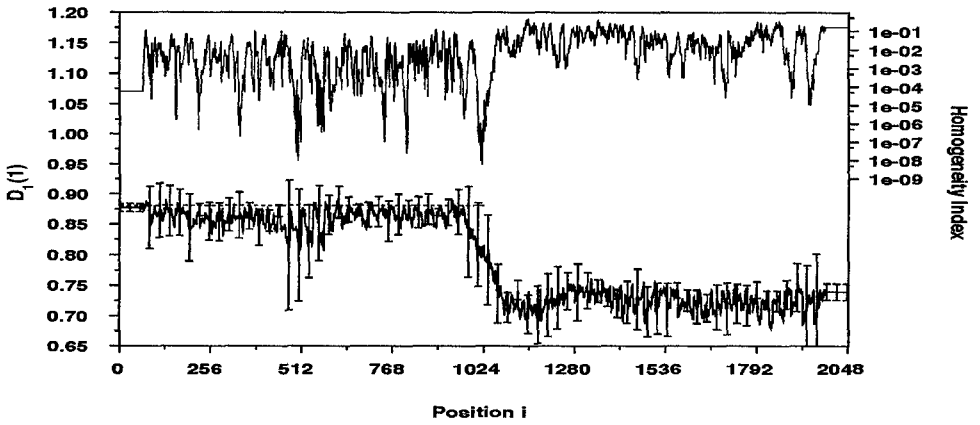


Figure 9: $D_1(i)$ without any homogeneity correction. The dashed line is the theoretical value of $D(1)$.

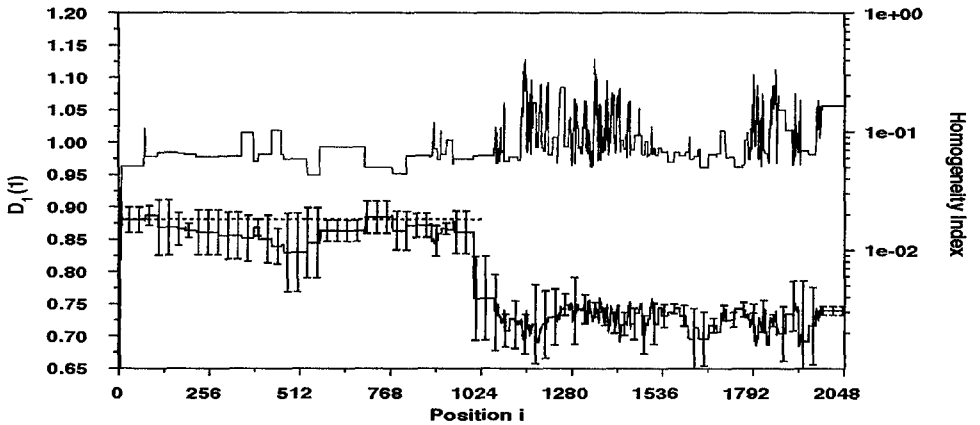


Figure 10: Same than Fig. 10, but with the homogeneity correction at level 0.05.

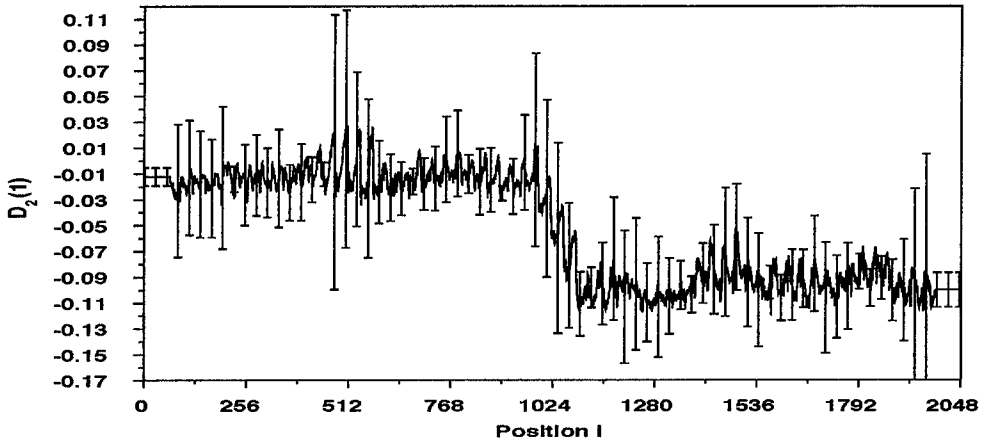


Figure 11: $D_2(l)$ without any homogeneity correction.

7 Conclusions

For signals that are *nearly* piecewise stationary, our method for generating textural transforms results in a sharper detection of the boundary between distinct segments. Indeed, the uncertainty on the location of the transition is much smaller than the window size. These improvements have been obtained in the context of approximately piecewise stationary signals. The special cases examined were the local average of a white noise and the generalized dimensions $D_n(q)$ of adjacent binomial measures. A better assessment of the algorithm proposed should involve segmentation tests in the presence of different types of noise, e.g. colored noise, long-tailed distribution noise, as well as real signals such as 1-d cuts through images.

It is emphasized that our method is quite general and can be used for any statistical parameter. Applied to the GMA representation, we demonstrated that the generalized dimensions $D_n(q)$ can clearly detect departures from multifractality^d in a signal, while providing the analogue of the classical generalized dimension $D(q)$ for multifractals.

References

1. Haralick R.M., 1986. "Statistical Image Texture Analysis", In: Handbook of Pattern Recognition and Image Processing, Chapter 11, T. Young and K. S. Fu, (eds.), Orlando, Florida: Academic Press, 247--279.
2. A. Saucier, O. K. Huseby, and J. Muller, 1997: Electrical texture characterization of dipmeter microresistivity signals using multifractal analysis. *Journal of geophysical research*, 102:10327-10337.
3. Saucier, A. and J. Muller, 1999. A Generalization of Multifractal Analysis Based on Polynomial Expansions of the Generating Function. In: "Fractals: Theory and Applications in Engineering". Dekking, Lévy Véhel, Lutton, Tricot (eds.), Springer, London. 81-91.

^d Multifractality is used here in the classical sense of a linear behavior of the generating function $\chi_q(\delta)$ plotted as a function of a scale parameter δ on log-log coordinates.

4. Haralick R.M., 1975. "A Resolution Preserving Textural Transform for Images", Proceedings of the IEEE Computer Society Conference on Computer Graphics, Pattern Recognition, and Data Structure San Diego, California, May 14--16, 51--61.
5. P. C. Chen and T. Pavlidis, 1978. Segmentation by texture using a co-occurrence matrix and a split-and-merge algorithm, *Tech. Rep. 237*, Princeton University, Princeton, New Jersey.
6. A. K. Jain and F. Farrokhnia, 1991. Unsupervised texture segmentation using Gabor filters. *Patt. Recogn.*, 24(12):1167-1186.
7. M. Porat and Y. Zeevi. January 1989. Localized texture processing in vision: analysis and synthesis in Gaborian space. *IEEE Trans. Biomed. Eng.*, 36(1): 115-129.
8. M. Unser, November 1995. Texture classification and segmentation using wavelet frames. *IEEE Trans. Image Proc.*, 4(11):1549-1560.
9. Stéphane Mallat, 1998. A wavelet tour of signal processing. Academic press, London.
10. K. S. Chen, S. K. Yen and D. W. Tsay, 1997. Neural classification of SPOT imagery through integration of intensity and fractal information. *Int. J. Remote Sensing*, 18(4): 763-783.
11. T. R. Reed and J. M. Hans du Buf, May 1993. A Review of Recent Texture Segmentation and Feature Extraction Techniques. *CVGIP: Image Understanding*, 57(3):359-372.